

REGIONAL SEISMIC FOCAL DEPTH ESTIMATION IN COMPLEX TECTONIC ENVIRONMENTS

Anastasia Stroujkova¹, Delaine T. Reiter¹, and Robert H. Shumway²

Weston Geophysical Corporation¹ and University of California, Davis²

Sponsored by National Nuclear Security Administration
Office of Nonproliferation Research and Development
Office of Defense Nuclear Nonproliferation

Contract No. DE-FG02-03ER83820

ABSTRACT

The accurate estimation of the depth of small, regionally recorded events continues to be an important and difficult monitoring research problem. In our previous work we developed a combined regional depth estimate, which represents a weighted average of multiple independent measurements of event depths. Our combined measurement includes focal depths found through assisted array processing of early *P*-wave coda, surface-wave amplitude inversions, and hypocenters estimated from regional travel times. We performed an initial validation of our methodology by applying it to moderate-sized events located within regional distances of the KSAR (Wonju, South Korea) teleseismic array. Our study in Korea showed that the new method produced accurate and consistent depth estimates using regional data. We also found that the IASPEI91 global reference velocity model was appropriate for the relatively simple tectonic region within regional distances of the KSAR array.

In this study we further investigate the validity of our regional depth estimator in a more tectonically complex area, specifically in the region around the array in Turkey (Keskin; BRAR/BRTR). The region surrounding the BRAR/BRTR array is dominated by the continental collision between the Eurasian, African and Arabian plates. In a complicated tectonic zone such as this, a global reference velocity model may not adequately predict the regional travel times and amplitudes of observed regional phases, which can potentially lead to poor focal depth estimates. To address this issue we have examined the sensitivity of the depth estimator to the velocity model used in the analyses. We have applied the depth estimator to regional data from well-located events in the Middle East for the IASPEI91 reference and two regional velocity models. Our results indicate that a poorly chosen velocity model can produce inconsistencies between the individual technique depth estimates. However, the depth estimator is less sensitive to the velocity model than might be expected; i.e., in many cases we show good correlation between our regional depth estimator results obtained using different velocity models.

OBJECTIVE

We have developed a technique that statistically combines measurements from regional data into a single focal depth estimator. Our continuing research objective is to validate the technique in a variety of tectonic environments by systematically testing the behavior and robustness of our regional depth estimator with well-recorded, moderate sized events from different regions of nuclear monitoring concern. In this study we report on results calculated from events in the region surrounding the regional array in Keskin, Turkey (BRAR/BRTR).

RESEARCH ACCOMPLISHED

The study area surrounding the Keskin (BRAR/BRTR) array in Turkey represents a 1000-km-wide zone of continental collision between the Eurasian, African and Arabian plates. The region east of the Keskin array (Turkey and Western Iran) is composed of several distinct seismotectonic areas, shown in Figure 1.

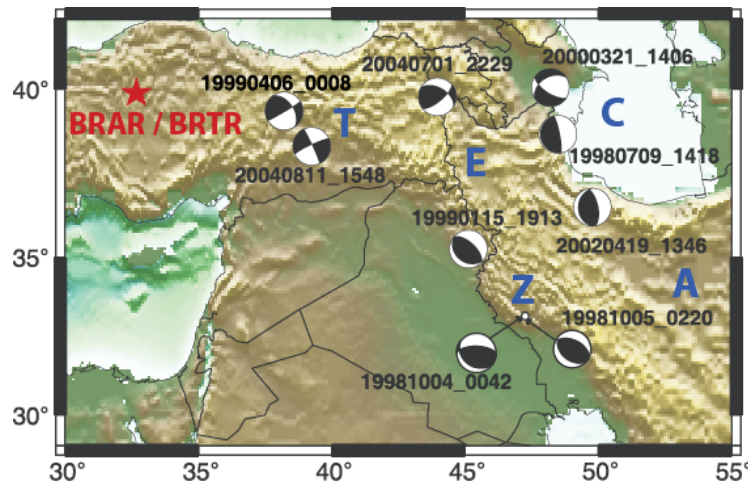


Figure 1. Map showing tectonic features (blue letters), locations and focal mechanisms of study events, and the BRAR/BRTR array in Turkey (red star). The geographic and tectonic features indicated with blue letters include Turkey (T), Eastern Iran (E), Alborz mountains (A), Central Caspian (C), and Zagros mountains (Z).

Each tectonic region shown in Figure 1 exhibits a characteristic pattern of focal depth distribution. In a recent study Engdahl et al. (2006) described several general patterns of earthquake focal depths using a revised version of the Engdahl, van der Hilst and Buland (EHB) location database (Engdahl et al., 1998). The patterns they observed can be described as follows:

1. **Region T:** Seismicity in Turkey is dominated by strike-slip focal mechanisms, which are concentrated between depths of 10–20 km.
2. **Region E:** Seismicity in Eastern Iran is in the upper crust, shallower than ~20 km, with a median depth of 12 ± 5 km.
3. **Region Z:** In the Zagros fold-and-thrust region, most of the earthquakes are shallower than 30 km, with median depth of 15 ± 7 km.
4. **Region C:** Central Caspian seismicity follows the Apsheron-Balkhan Sill, resulting in a depth range of 30–100 km that deepens toward the north.
5. **Region A:** Seismicity in the Alborz region in Northern Iran is distributed through the crust, with a median depth of 20 ± 8 km.

According to Engdahl et al. (2006), the uncertainty of the focal depth estimates reported in the revised EHB database is ~10 km, which is sufficiently accurate to allow differentiation between the various tectonic subregions. In our validation study we have taken advantage of the seismic focal depth distributions described by Engdahl et al. (2006) to provide additional constraints on depths predicted by the estimator. In Figure 1 we also show the sample

subset of events we have studied thus far in the region to the east of the BRAR/BRTR array. We have applied our depth estimator technique to nine events that fall into each of the tectonic categories described above. The selected events sample most of the subregions described above. The main criteria for an event’s selection were: 1) proximity to the Keskin array; and 2) high-quality bulletin locations and moment-tensor solutions from the Harvard Centroid Moment Tensor (CMT) catalog (Dziewonski et al., 1981). Table 1 lists the International Seismic Centre (ISC) coordinates and Harvard CMT magnitudes of the events in our study. We note that the ISC depths are in many cases significantly deeper than the regional lower depth limits predicted from other studies, including the database in Engdahl et al. (2006).

Table 1. Location parameters from our Turkey regional earthquake study database. A designation of ‘d’ in the ISC depth column indicates that the hypocenter solution was allowed to range freely in depth, while ‘f’ indicates that the depth was fixed in the hypocenter estimate. The column labeled ‘pP_DEPTH’ is the ISC composite depth from teleseismic pP-P phase observations.

Event ID (Origin Date)	Lat. °N	Long. °E	ISC Location Depth (km)	pP_DEPTH (km)	Tectonic Region	Mw	Distance to BRAR, °
19980709_1418	38.60	48.48	55.4 d	39 ± 3	C	5.9	12.18
19981004_0042	33.23	47.20	24.9 d	22 ± 4	Z	5.3	13.35
19981005_0220	33.24	47.24	18.1 d	30 ± 3	Z	5.4	13.37
19990115_1913	35.25	45.13	59.2 d	55 ± 3	Z	5.1	10.80
19990406_0008	39.37	38.21	30.7 d	11 ± 2	T	5.4	4.23
20000321_1406	40.05	48.20	77.6 d	60 ± 1	C	5.1	11.13
20020419_1346	36.52	49.77	38.8 d	32 ± 6	C	5.2	13.1
20040701_2229	39.78	43.97	5.0 f	18 ± 2	E	5.1	7.98
20040811_1548	38.34	39.25	7.4 f	14 ± 1	T	5.6	4.57

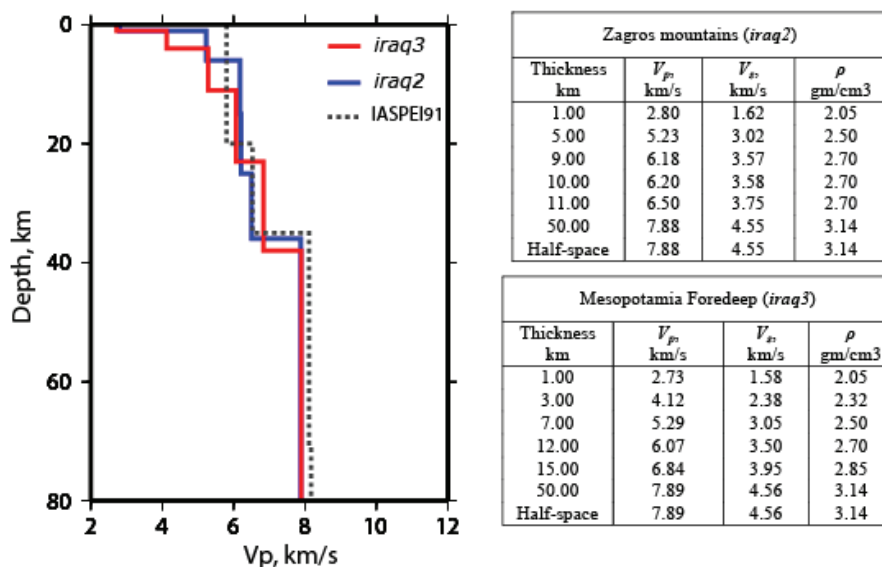


Figure 2. Left: velocity versus depth plots for the models used in the study, including the IASPEI91 reference model, Zagros Mountains (*iraq2*) and Mesopotamia Foredeep (*iraq3*). Right: velocity and density values versus layer thickness for the *iraq2* and *iraq3* models.

The region to the east of the BRAR/BRTR array is suitable for our goal of studying the behavior of our depth estimator in various observational settings, because the velocity structure to the east of the BRTR array is highly heterogeneous and poorly constrained. For our subset of events to the east of the BRTR array, we compared the results of the estimator using the IASPEI91 reference model (Kennett and Engdahl, 1991) and two 1-D regional

velocity models developed for Iraq (Figure 2). The *iraq2* model was developed by Al-Eqabi (2007) for the Zagros mountains in Northern Iraq, and the *iraq3* model (Al-Eqabi, 2007) was developed for Mesopotamia Foredeep from South Turkey to Baghdad. The *iraq2* and *iraq3* models have slightly lower velocities below the Moho than IASPEI91, which contradicts some velocity studies in the area (e.g., Hatzfeld et al., 2003). In another study (Doloei and Roberts, 2003), receiver functions predicted the presence of a low-velocity layer below the Moho. However, travel-time tables that include a low-velocity layer lead to shadow zones in some distance ranges. The lowering of the upper-mantle velocity in the *iraq2* and *iraq3* models is a simple way to avoid ray-tracing complications.

The Regional Depth Estimator

To develop a regional depth estimator, we combine several measures related to depth d_i ; ($i = 1, 2, \dots, n$) and their standard errors σ_i into an overall estimator for the depth of an event (Draper and Smith, 1998). The estimator is constructed by a statistical averaging of the n independent observations of depth:

$$\hat{D} = \left(\sum_{i=1}^n \frac{1}{\sigma_i^2} \right)^{-1} \sum_{i=1}^n \frac{d_i}{\sigma_i^2}, \quad (1)$$

with an estimated standard deviation given by

$$\sigma_{\hat{D}} = \sqrt{\left(\sum_{i=1}^n (1/\sigma_i^2) \right)^{-1}}. \quad (2)$$

The simplification in Equation 1 implies that \hat{D} , which combines a variety of individual measurements, requires knowledge of the standard errors associated with each measurement method. We emphasize that this type of statistical averaging is only valid for *independent* depth estimates; i.e., measurements that are not shared between the methods.

In our current formulation of the estimator, we incorporate three independent depth measurement methods. The first depth measurement is directly estimated from regional depth-phase delays ($pPn-Pn$ and $sPn-Pn$) determined using an Enhanced Cepstral F-Statistic Method (ECFSM; Stroujkova and Reiter, 2006). We derive our second independent depth measurement from the hypocenter found in a sparse-network location of catalog Pn and Sn arrivals supplemented by analyst-derived pPn and/or sPn arrival times. Our third depth measurement is derived from the inversion of regional surface-wave spectral amplitudes (SWA). In the following sections we provide details on the application of the individual methods to the events in our study database.

Depth Measurement 1: Enhanced Cepstral Processing

The travel-time delay between a primary arrival and its reflection from the Earth's surface (e.g., $pPn-Pn$ or $sPn-Pn$) can be directly converted to a source depth using a velocity profile near the source position. Cepstral methods can be used to find these time delays through analysis of the periodicity in log spectra (Bogert et al., 1963, Oppenheim and Schaffer, 1975). However, cepstral methods, including the Cepstral F-Statistic Method (CFSM, Bonner et al., 2002), are not a reliable way to identify depth-phase delays at regional distances, because they produce multiple false detections. Additional evidence must therefore be used to verify whether phases detected by the CFSM are actual depth phases. We currently estimate the apparent velocities, amplitudes and frequency content of both the direct arrival and suspected surface reflections to help confirm (or decisively eliminate) the cepstral detections of regional depth-phase arrivals. These phase characteristics can be found using multiple methods such as MULTiple Signal Classification (MUSIC) (e.g., Schmidt, 1979; Schissle et al., 2004), and cross-correlation analysis (e.g., Cansi, 1995), both of which produce phase characteristic estimates with sufficient accuracy and resolution. We are calling this revised method of analysis the ECFSM.

To calculate the standard error needed by our depth estimator for the ECFSM, we use an *ad hoc* method (Stroujkova and Reiter, 2006) to examine up to six of the largest peaks above the 99% confidence level found in the cepstral F statistic. If a peak is determined to be a phase arrival with a velocity and back azimuth similar to the Pn arrival, it is

retained for further analysis. To be defined as similar, an arrival's velocity estimate using the MUSIC estimator must be within 0.5 km/s of the Pn estimate and the back azimuth within 10° for high signal-to-noise ratio (SNR) data (1.0 km/s and 15° for poor SNR). Then we assume the delay time at a particular peak can be either a sPn or a pPn arrival, and compute the sPn and pPn depths associated with the delay time using the background velocity model. The final depth and standard error are computed as the average and standard deviation of all the viable sPn and pPn depths. This method provides a worst-case estimate of the depth and standard error, but eliminates the requirement that the analyst decide which arrival among many possibilities is a particular depth phase.

Using the above approach, we applied the ECFSM (using cross-correlation to determine the confirming phase characteristics) to calculate the event depths and standard errors of the events in Table 1. Figure 3 shows two examples of the ECFSM and cross-correlation results applied to the BRAR/BRTR short-period data. In the left set of panels, we show the results from Event 20040811_1548, which is a strike-slip event in Region T. There is one peak in the cepstra (2nd subplot from the top) that is reflected in the F statistic (it is important that both the cepstra and the F statistic are peaked at the same time), which is confirmed by the cross-correlation analysis in the bottom three subpanels. We confirm a phase arrival in the cross-correlation analysis by identifying a stable velocity and back-azimuth occurring over a 2-3 second time window, accompanied by a low value of root-mean-square (RMS) residuals. In order to maintain a fairly smooth appearance of the cross-correlation results, the processing window is 2.3 seconds in length. The final results for Event 20040811_1548 indicate a pPn arrival at an approximately 9-second delay.

In the right set of subpanels of Figure 3, we show the ECFSM results from Event 20020419_1346, which occurred in the south portion of Region C (Caspian). Waveforms from this region are notoriously difficult to analyze (e.g., Mangino and Priestley, 1998), but the results we found with ECFSM are fairly straightforward to interpret for this particular event. The cepstra and F statistic reveal two significant peaks that are consistent with pPn and sPn arrival characteristics in the cross-correlation results.

There is no velocity model involved in the initial portion of the cepstral analysis: it is a signal processing technique that produces only the travel-time delays and statistical likelihood of the presence of a phase echo. In the enhanced portion of the cepstral analysis we convert the estimated time delays to a depth plus associated standard error using each of the three velocity models we compared in our study. The results of these calculations can be found in Table 3 for the events in Table 1.

Depth Measurement 2: Sparse-Network Regional Hypocenter Estimation

To determine our second independent depth measurement, we compute event hypocenters using the GMEL software package (Rodi, 2006). GMEL (an acronym for Grid-search Multiple-Event Location) finds solutions to the multiple-event location problem using a grid search to find the best-fitting location parameters (origin times, hypocenters, and travel-time corrections) and associated error estimates from a set of arrival time data measured from multiple events, stations and seismic phases. In this study we ran GMEL in single-event mode; that is, the case in which the event locations and the origin times are the only unknowns. While the events in our study were all observed teleseismically, we limited the arrival-time data in our relocations to travel times from stations within 17° from each event.

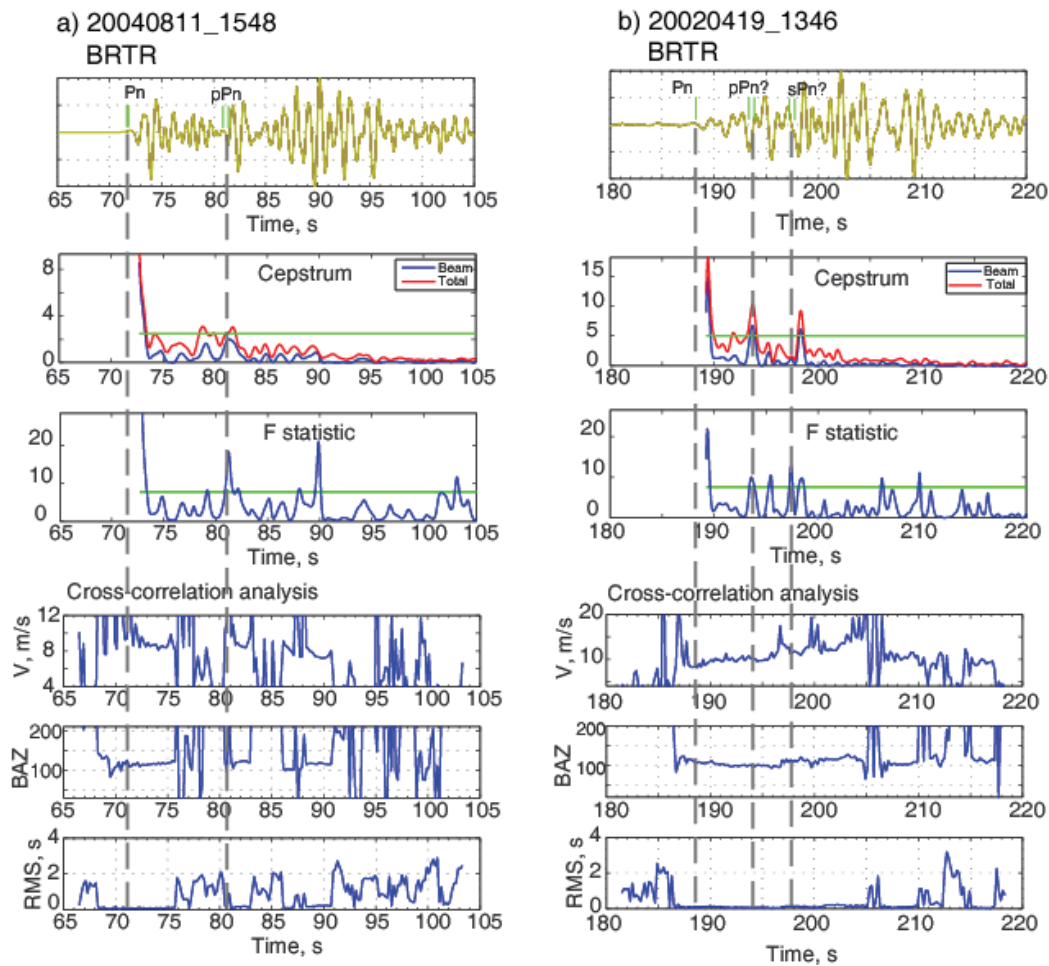


Figure 3. Examples of ECFSM and cross-correlation array processing applied to study events: a) Event 20040811_1548 and b) Event 20020419_1346. The top subplot shows array beam; second subpanel shows the beam and total cepstra from the CFMS; and the third subpanel shows cepstral F Statistic with a green line at the 99% significance level. The bottom three subpanels show the results of the cross-correlation analysis, including apparent horizontal velocity, back azimuth and the RMS error.

The majority of the arrival data included in the GMEL runs came from the ISC catalog. However, to constrain the GMEL hypocenter depths we supplemented catalog Pn and Sn arrival times with analyst picks of regional depth-phase arrival times. We picked candidate depth-phase arrivals at the available regional three-component (3-C) broadband stations and confirmed those picks using polarization analysis. To ensure the independence of focal depths estimated using GMEL from those estimated via the enhanced CSFM, we did not include any arrivals observed at BRTR in the GMEL runs.

Table 2 shows the summary of the GMEL relocation results, which indicate that the choice of velocity model did not significantly affect the depths retrieved by the GMEL hypocenter relocation. In every case but one for which the ISC allowed a free-depth solution, the GMEL depth was shallower. In both of the fixed-depth cases, the GMEL depth was slightly deeper.

Table 2. Results obtained by GMEL for events in Table 1 using different velocity models.

Event ID	Number of Phase Arrivals		Network Secondary Azim. Gap (°)	<i>iasp91</i>		<i>iraq2</i>		<i>iraq3</i>	
	<i>Pn</i>	<i>pPn</i> & <i>sPn</i>		Epicenter shift, km	Depth shift, km	Epicenter shift, km	Depth shift, km	Epicenter shift, km	Depth shift, km
19980709_1418	85	3	119	26.1	-22.1	18.6	-22.1	18.7	-22.1
19981004_0042	74	0	113	8.9	-24.9	11.5	-24.8	10.4	-24.9
19981005_0220	64	4	114	17.5	-1.1	18.1	-0.7	18.1	-7.0
19990115_1913	53	0	80	0.9	-59.2	4.9	-26.2	4.7	-36.7
19990406_0008	93	1	64	9.0	-27.0	12.8	-19.6	12.4	-19.6
20000321_1406	38	10	107	27.3	-45.1	32.5	-44.3	32.0	-54.5
20020419_1346	28	3	135	31.8	-35.1	27.4	-35.1	28.1	-35.1
20040701_2229	92	1	105	17.8	22.9	8.0	25.9	7.9	12.5
20040811_1548	85	5	118	7.8	0.5	9.1	3.7	8.0	3.7

Depth Measurement 3: Inversion of SWA

For the third independent depth measurement included in the depth estimator, we invert the spectral amplitudes of Rayleigh and Love waves for event depth and focal mechanism using source inversion codes (Herrmann and Ammon, 2002). The software performs a grid search over a model space of moment M_0 , focal depth h , and mechanism (strike ϕ , dip δ , and rake λ) to minimize the misfit between observed and predicted surface-wave amplitude spectra. The input required for the inversion consists of the spectral amplitudes of the fundamental Rayleigh and Love waves from a set of regional stations and a 1-D regional Earth model.

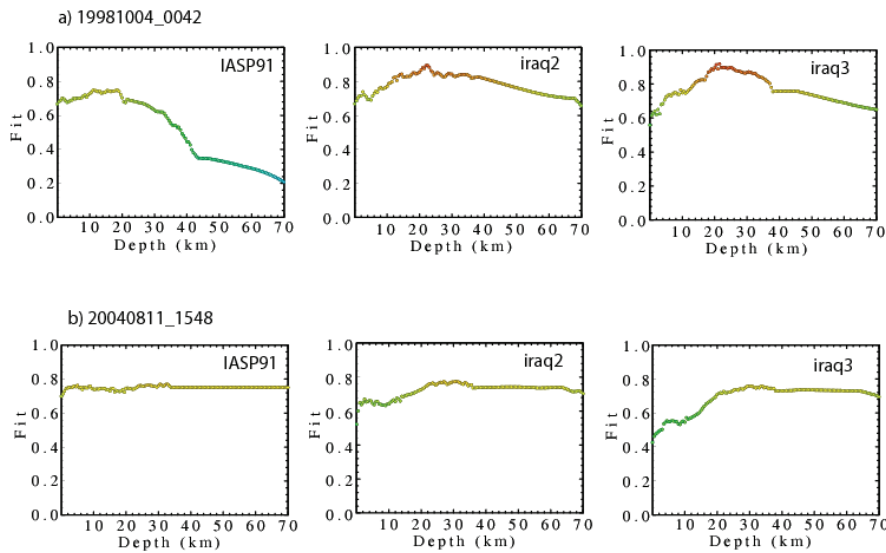


Figure 4. Examples of depth confidence levels calculated from surface-wave amplitude inversion for a) Event 19981004_0042 and b) Event 20040811_1548. Results are shown for the three velocity models described earlier: IASPEI91 (left panels), *iraq2* (middle panels) and *iraq3* (right panels). The best depth estimate corresponds to the maximum value of the fit function.

To derive the surface-wave amplitude spectra for the inversion, we applied multiple-filter analysis (Herrmann, 1973; Bhattacharya, 1983) to surface waves observed at regional distances from our study events. We then ran the inversion method to estimate the depths and focal mechanisms for the nine events listed in Table 1 using the IASPEI91 reference model and the processed spectral-amplitude data. We estimate the standard error on depths

from the surface-wave spectral amplitude inversions using a jack-knife method. This involves repeating the inversion $N-1$ (where N equals the number of stations) times, leaving one of the stations out during each calculation. Table 3 shows the average depth and its standard deviation that were calculated from all the inversion results.

Figure 4 shows an example of the inversion fit with respect to depth for Events 19981004_0042 and 20040811_1548 using the different velocity models. The fit functions for Events 19981004_0042 show well-defined maxima for all of the velocity models. In contrast, the fit functions for Event 20040811_1548 have broader maxima, with the IASPEI91 model producing the least defined peak. This broader fit function is reflected in the higher value of depth uncertainty ($\sigma_{swa} = 9.8$ km) computed for Event 20040811_1548 using the IASPEI91 model.

Summary of Regional Depth Estimator Results

Table 3 summarizes the results of the application of our depth estimator approach to the study events in Table 1. For each event we include the results comparing the three velocity models: IASPEI91, *iraq2* and *iraq3*. There are several observations that can be made regarding the correlation between the different individual estimates. First, we note that the new estimator depths correlate quite well with depths expected for each event's tectonic region (as described in Engdahl et al., 2006). We also find that all of the ISC free-depth solutions and composite pP_DEPTH estimates are much deeper than the depths found with our new estimator .

Secondly, there is a high degree of correlation between the depths estimated with ECFSM and SWA. Correlation coefficients calculated between the ECFSM and SWA methods are high for all velocity models (0.80, 0.89 and 0.94 for IASPEI91, *iraq2* and *iraq3* respectively). This is consistent with a high correlation between the ECFSM and SWA methods we found in our previous study of events in the Korean Peninsula and eastern China.

We also observe that in some cases the three individual methods produce significantly different estimates with tightly constrained standard errors (small σ_i 's), resulting in a weighted combination (estimator) that is not meaningful (c.f. Events 19981004_0042 and 19990115_1913). We have observed this undesirable feature of the depth estimator in prior studies and plan to improve the statistical estimator to eliminate this type of occurrence. For the current data set the largest number of these inconsistencies occurred with the *iraq3* velocity model.

The results in Table 3 indicate significant variability between the individual depth estimates for a given event, depending on the velocity model used, particularly for the GMEL and SWA methods. However, the estimator depth values are very similar across the various velocity models. The correlation coefficients between the results obtained using different velocity models are: $C_{IASPEI91-iraq2} = 0.96$, $C_{IASPEI91-iraq3} = 0.91$, and $C_{iraq2-iraq3} = 0.90$. These values are quite high, which indicates that the new estimator is not strongly sensitive to the velocity model. Of course this observation may not hold true in regions where there is strong regional variation in velocity-sensitive parameters such as crustal thickness, which for the current study remained fairly constant across the three velocity models studied.

Table 3. Summary of depth estimator results. Results for the individual depth-estimation methods as well as the new combined estimator (bolded columns) are shown for the three velocity models IASPEI91, *iraq2* and *iraq3*.

19980709_1418	55.4 d	IASPEI91	29	1.9	22.3	8.3	33.3	5.4	29.2	1.8
		<i>iraq2</i>	28	1.9	23.1	9.1	33.3	6	28.3	1.8
		<i>iraq3</i>	36.5	1.9	13.9	5.1	33.3	6.5	33.7	1.7
19981004_0042	24.9 d	IASPEI91	18.5	1.9	7.8	2.6	0	8.6	14.3	1.5
		<i>iraq2</i>	22.5	2.3	7	2.8	0	26.3	16.2	1.8
		<i>iraq3</i>	21.5	7.1	4.5	1.1	0	38.3	4.9	1.1
19981005_0220	18.1 d	IASPEI91	11	1.1	8.7	0.5	17	4	9.3	0.4
		<i>iraq2</i>	22.5	2.3	7	2.8	17.4	2.9	14	1.5
		<i>iraq3</i>	13	5.6	5.1	0.9	16.8	3.2	6.1	0.9
19990115_1913	59.2 d	IASPEI91	16.5	1.8	15.4	0.4	0	54.8	15.5	0.4
		<i>iraq2</i>	16.5	2.9	15.4	0.4	33	104.9	15.4	0.4
		<i>iraq3</i>	22	3.8	9.6	0.6	22.5	91.7	9.9	0.6
19990406_0008	30.7 d	IASPEI91	17	1.7	11.9	1.3	3.7	4.4	13.3	1
		<i>iraq2</i>	24	6.1	11.5	1.4	11.1	7.5	12	1.3
		<i>iraq3</i>	24	6.1	7	1.4	11.1	5	8.1	1.3
20000321_1406	77.6 d	IASPEI91	34.5	1.3	43	2.9	32.5	1.9	35	1
		<i>iraq2</i>	68.5	6.2	38	2.9	33.3	2	37	1.6
		<i>iraq3</i>	62	6.9	30	3	23.2	1.8	26.8	1.5
20020419_1346	38.8 d	IASPEI91	3.5	2.2	10.9	0.6	3.7	3.2	10.2	0.6
		<i>iraq2</i>	6	3	10.5	0.6	3.7	2.7	10	0.6
		<i>iraq3</i>	10.5	4.1	6.9	0.4	3.7	1.9	6.8	0.4
20040701_2229	5.0 f	IASPEI91	16	4.6	5.4	0.6	27.9	5.6	5.8	0.6
		<i>iraq2</i>	11.5	2.8	4.6	0.5	30.9	8.2	4.9	0.5
		<i>iraq3</i>	19	1.4	3.2	0.3	17.5	3.5	4	0.3
20040811_1548	7.4 f	IASPEI91	30.5	9.8	24	2.6	7.9	2.1	14.7	1.6
		<i>iraq2</i>	31	1.9	24.8	2	11.1	2.5	24.1	1.2
		<i>iraq3</i>	30	2.6	15.4	2.8	11.1	1.8	16.8	1.3

CONCLUSIONS AND RECOMMENDATIONS

In our previous validation experiment of the regional depth estimator approach in the region of eastern China and South Korea (Stroujkova and Reiter, 2006), we demonstrated excellent success in producing correlated and consistent depths between the individual methods included in the combined estimator. As a consequence, the estimator produced tightly constrained estimates of the depths of earthquakes in our data set. One potential reason for the successful application of our approach in Korea was the fairly homogeneous nature of the tectonic features within regional distances of the events in our study. This allowed us to use a simple 1-D reference model for all of our calculations, rather than incorporating more complex velocity models to produce better data fits in each estimation method.

In this study we examined the validity of the estimator in another, more complex regional setting. Our goal was to determine how robust the method is when the tectonic complexity (and potential lack of data fit to a single reference velocity model) increases. Based on our initial results we conclude that various individual depth-estimation methods have different degrees of sensitivity to the velocity model used in computations. A good correlation observed between the estimates obtained with different velocity models is a promising result. In addition, our depth estimate is in a good agreement with the pattern of focal depth distribution in the region (Engdahl et al., 2006). We find that the depths reported in the ISC catalog tend to be significantly overestimated (e.g., Table 1).

While we acknowledge the limited size of the database we have examined to date in the region around Turkey, we have found that the new estimator can provide robust depth estimates from regional data in a tectonically complex

region. In future work we will continue to apply the new estimator in different tectonic settings. We will also address some of the short-comings of the method, such as the need for improvement in the statistical behavior of the estimator, which is currently a fairly simple weighted average.

REFERENCES

- Al-equabi, G. I. Personal Correspondence. 2007.
- Bhattacharya, S. N. (1983). Higher order accuracy in multiple filter technique, *Bull. Seism. Soc. Am.* 73: 1395–1406.
- Bogert, B. P., M. J. R. Healy and J. W. Tukey (1963), The quefrency analysis of time series for echoes: cepstrum, pseudo-autocovariance, cross-cepstrum and saphe cracking, in *Proceedings of a Symposium on Time Series Analysis*, ed. M. Rosenblatt, John Wiley and Sons, Inc., New York.
- Bonner, J. L, D. T. Reiter, and R. H. Shumway (2002), Application of a cepstral F statistic for improved depth estimation, *Bull. Seism. Soc. Am* 92: 1675–1693.
- Cansi, Y. (1995). Earthquake location applied to a mini-array: K-spectrum versus correlation method, *Geophys. Res. Lett.* 20: (17), 1819–1822.
- Crotwell, H.P., T.J. Owens, and J. Ritsema (1999). The TauP Toolkit: Flexible seismic travel-time and ray-path utilities. *Seism. Res. Ltrs.*, 70, 154–160.
- Doloei, J. and R. Roberts (2003). Crust and uppermost mantle structure of Tehran region from analysis of teleseismic P-waveform receiver functions, *Tectonophysics* 364: 115–133.
- Draper N. R. and H. Smith (1998). *Applied Regression Analysis* (3rd edition). New York: Wiley.
- Dziewonski, A. M., T.-A. Chou, and J. H. Woodhouse (1981). Determination of earthquake source parameters from waveform data for studies of global and regional seismicity, *J. Geophys. Res.* 86: 2825–2852.
- Engdahl, E.R., R.D. van der Hilst, and R.P. Buland, 1998, Global teleseismic earthquake relocation with improved travel times and procedures for depth determination, *Bull. Seism. Soc. Am.* 88: 722–743.
- Engdahl, E.R., J. Jackson, S. Myers, E. Bergman, and K. Priestley (2006). Relocation and assessment of seismicity in Iran region, *Geophys. J. Int.* 167: 761–778.
- Hatzfeld, D., M. Tatar, K. Priestley, and M. Ghafory-Ashtiany (2003). Seismological constraints on the crustal structure beneath the Zagros Mountain belt (Iran), *Geophys. J. Int.* 155: 403–410.
- Herrmann, R., and C. Ammon, (2002). Surface waves, receiver functions and crustal structure. In *Computer programs in seismology*.
- Kennett B. L. N., and E. R. Engdahl (1991), Travel times for global earthquake location and phase identification, *Geophys. J. Int.* 105: 429–465.
- Mangino, S., and K Priestley (1998). The crustal structure of the southern Caspian region, *Geophys. J. Intl.* 133 (3): 630–648.
- Oppenheim, A. V., and R. W. Schafer (1975). *Digital Signal Processing*. New York: Prentice Hall.
- Rodi, W. (2006). Grid-search event location with non-Gaussian errors, *Phys. Earth & Planet. Int.* 158 (1): 55–66.
- Schisselé, E., J. Guilbert, S. Gaffet, and Y. Cansi (2004). Accurate time-frequency-wavenumber analysis to study coda waves, *Geophys. J. Intl.* 158: (2), 577–591.

29th Monitoring Research Review: Ground-Based Nuclear Explosion Monitoring Technologies

- Schmidt, R.O. (1979). Multiple emitter location and signal parameter estimation. *Proc. RADC Spectral Estimation Workshop*, 243–258, Rome, Italy.
- Stroujkova, A. and D. Reiter (2006). Regional Depth Phase Detection and Focal Depth Estimation: Application to Events in Southeast Asia, in *Proceedings of the 28th Seismic Research Review: Ground-Based Nuclear Explosion Monitoring Technologies*, LA-UR-06-5471, Vol. 1, pp. 520–529.